Proceedings of ALGORITMY 2024
pp. 129–138

EVOLUTION OF MULTIPLE CLOSED KNOTTED CURVES IN SPACE

MIROSLAV KOLÁŘ * AND DANIEL ŠEVČOVIČ †

Abstract. We investigate a system of geometric evolution equations describing a curvature driven motion of a family of 3D curves in the normal and binormal directions. We explore the direct Lagrangian approach for treating the geometric flow of such interacting curves. Using the abstract theory of nonlinear analytic semi-flows, we are able to prove local existence, uniqueness, and continuation of classical Hölder smooth solutions to the governing system of non-linear parabolic equations modelling n evolving curves with mutual nonlocal interactions. We present several computational studies of the flow that combine the normal or binormal velocity and considering nonlocal interaction.

Key words. Curvature driven flow, binormal flow, nonlocal flow, Biot-Savart law, interacting curves, analytic semi-flows, Hölder smooth solutions, flowing finite volume method.

AMS subject classifications. 2010 MSC. Primary: 35K57, 35K65, 65N40, 65M08; Secondary: 53C80.

1. Introduction. In this work, we focus on the evolution of space curves involving interactions. These one-dimensional structures, which form space curves, are frequently encountered in various scientific and engineering challenges. Connections to dislocation dynamics are discussed in [10, 11] along with additional references. Historical research into the dynamics of vortex structures and rings, which align with one-dimensional curves, was initiated by Helmholtz [16]. The significance of vortex structures in aerospace technology is highlighted in several foundational studies (refer to Thomson [29], Da Rios [24], Betchov [6], Arms and Hama [3], and Bewley [7]). Vortex structures are known to maintain stability over time. This stability is evident in studies of tornadoes and descriptions of volcanic activities (see Fukumoto *et al.* [13, 14], Hoz and Vega [18], Vega [30]). Specific interactions between linear vortex structures, exhibiting dynamic behaviors such as 'frog leaps', are noted (refer to Mariani and Kontis [21]). For an overview of vortex dynamics and further discussions on the evolution of closed curves, please see our latest publication [9] by Beneš, Kolář, and Ševčovič.

The structure of the paper is as follows. Section 2 revisits the Lagrangian framework for evolving curve families. It introduces a set of evolutionary equations governing the dynamics of interacting curve systems, together with recent findings on the existence and uniqueness of classical Hölder continuous solutions. The proof technique employs the abstract theory of analytic semi-flows in Banach spaces, due to Angenent [2, 1]. Section 3 concentrates on the numerical discretization approach, utilizing the flowing finite-volume method for spatial derivative discretization and the method of lines to address the resulting ODE systems. In Section 4 we present examples of the dynamics of interacting curves, with interactions shaped by the Biot-Savart nonlocal law, and discusses the development of 3D evolving knotted curves.

*Department of Mathematics, Faculty of Nuclear Sciences and Physical Engineering Czech Technical University in Prague, Trojanova 13, Prague, 12000, Czech Republic

†Department of Applied Mathematics and Statistics, Faculty of Mathematics Physics and Informatics, Comenius University, Mlynská dolina, 842 48, Bratislava, Slovakia. Corresponding author: `sevcovic@fmph.uniba.sk`

2. Lagrangian description of evolving curves. We investigate a family of curves $\{\Gamma_t, t \geq 0\}$ evolving in space $\mathbb{R}^3$. We employ the Lagrangian description of curves, in which a curve is described by the position vector $\mathbf{X} = \mathbf{X}(t,u)$ for $t \geq 0$ and $u \in I$, where $I = \mathbb{R}/\mathbb{Z} \simeq S^1$ is the unit circle. The curve Γ_t is then parameterized by $\Gamma_t = \{\mathbf{X}(t,u), u \in I\}$. The unit tangent vector $\mathbf{T}$ to Γ_t is defined as $\mathbf{T} = \partial_s \mathbf{X}$, where s is the unit arc-length parametrization defined by $ds = g du$ where $g = |\partial_u \mathbf{X}|$ is the relative local length of the curve. Here, $|\cdot|$ denotes the Euclidean norm. The curvature κ of a curve Γ_t is defined as $\kappa = |\partial_s \mathbf{X} \times \partial_s^2 \mathbf{X}| = |\partial_s^2 \mathbf{X}|$. If $\kappa > 0$, we can define the Frenet frame along the curve Γ_t with unit normal $\mathbf{N} = \partial_s^2 \mathbf{X}/\kappa$ and binormal vector $\mathbf{B} = \mathbf{T} \times \mathbf{N}$, respectively. More specifically, we focus on the analysis of the motion of a family of n closed 3D curves Γ_t^i, $i = 1, \dots, n$, evolving in normal and binormal directions. Curves Γ_t^i are described by position vectors $\mathbf{X}^i$ and they satisfy the following system of geometric evolution equations for $i = 1, \dots, n$:

$$\partial_t \mathbf{X}^i = a^i \partial_{s^i}^2 \mathbf{X}^i + b^i (\partial_{s^i} \mathbf{X}^i \times \partial_{s^i}^2 \mathbf{X}^i) + \mathbf{F}^i + \alpha^i \mathbf{T}^i, \qquad \mathbf{X}^i(\cdot, 0) = \mathbf{X}_0^i(\cdot), \tag{2.1}$$

which is subject to initial conditions at the origin $t = 0$ representing parametrization of the family of initial curves $\Gamma_0^i, i = 1, \dots, n$. Here $a^i = a^i(\mathbf{X}^i, \mathbf{T}^i) \geq 0$, and $b^i = b^i(\mathbf{X}^i, \mathbf{T}^i)$ are bounded and smooth functions of their arguments, $\mathbf{T}^i$ is the unit tangent vector to the curve and s^i is the unit arc-length parametrization of the curve Γ_t^i. The source forcing term $\mathbf{F}^i$ is assumed to be a smooth and bounded function. Here $\mathbf{F}^i = \mathbf{F}^i(\mathbf{X}^i, \mathbf{T}^i, \gamma^{i1}, \dots, \gamma^{in})$ is the forcing term and $\gamma^{ij} = \gamma^{ij}(\mathbf{X}^i, \Gamma^j)$ may depend on the position vector $\mathbf{X}^i \in \mathbb{R}^3$ and the entire curve Γ_t^j. Notice that equation (2.1) represents the system of geometric evolution equations $\partial_t \mathbf{X}^i = v_N^i \mathbf{N}^i + v_B^i \mathbf{B}^i + v_T^i \mathbf{T}^i$ where the normal v_N^i, binormal v_B^i and tangent velocity v_T^i are given by: $v_N^i = a^i \kappa^i + \mathbf{F}^i \cdot \mathbf{N}^i$, $v_B^i = b^i \kappa^i + \mathbf{F}^i \cdot \mathbf{B}^i$, and $v_T^i = \alpha^i + \mathbf{F}^i \cdot \mathbf{T}^i$.

As an example of nonlocal source terms $\mathbf{F}^i, i = 1, \dots, n$, one can consider a flow of $n = 2$ interacting curves evolving in 3D according to the geometric equations:

$$\begin{aligned} \partial_t \mathbf{X}^1 &= a^1 \partial_{s^1}^2 \mathbf{X}^1 + b^1 (\partial_{s^1} \mathbf{X}^1 \times \partial_{s^2}^2 \mathbf{X}^1) + \gamma^{12}(\mathbf{X}^1, \Gamma^2), \\ \partial_t \mathbf{X}^2 &= a^2 \partial_{s^2}^2 \mathbf{X}^2 + b^2 (\partial_{s^2} \mathbf{X}^2 \times \partial_{s^2}^2 \mathbf{X}^2) + \gamma^{21}(\mathbf{X}^2, \Gamma^1), \end{aligned}$$

where the nonlocal source term given by the following vector field

$$\gamma^{ij}(\mathbf{X}^i, \Gamma^j) = \oint_{\Gamma_t^j} \frac{(\mathbf{X}^i - \mathbf{X}^j(s^j)) \times \mathbf{T}^j(s^j)}{|\mathbf{X}^i - \mathbf{X}^j(s^j)|^3} ds^j$$

represents the Biot-Savart force measuring the integrated influence of points $\mathbf{X}^j$ belonging to the second curve $\Gamma_t^j = \{\mathbf{X}^j(u), u \in [0,1]\}$ at a given point $\mathbf{X}^i \in \Gamma_t^i$.

The tangential velocity α^i that appears in geometric evolution (2.1) has no impact on the shape of the evolving family of closed curves $\Gamma_t^i, t \geq 0$. This means that the curve $\Gamma_t^i, t \geq 0$, evolving according to (2.1) does not depend on a particular choice of the total tangential velocity $v_T^i = \mathbf{F}^i \cdot \mathbf{T}^i + \alpha^i$. On the other hand, the tangential velocity has a significant impact on the analysis of evolution of curves from both the analytical and numerical points of view (see e.g., Hou et al. [17], Kimura [20], Mikula and Ševčovič [26, 22, 23], Yazaki and Ševčovič [27]). Barrett *et al.* [4, 5], Elliott and Fritz [12], investigated the gradient and elastic flows for closed and open curves in $\mathbb{R}^d, d \geq 2$. They constructed a numerical approximation scheme using a suitable tangential redistribution. Kessler *et al.* [19] and Strain [28] illustrated the role of a suitably chosen tangential velocity in numerical simulation of two-dimensional snowflake growth and unstable solidification models. Garcke *et al.* [15] applied the uniform tangential redistribution in the theoretical proof of the non-linear stability of stationary solutions for curvature driven flow with triple junction in the plane.

It is known that the ratio g^i/L^i of the relative local length g^i and length $L^i = \int_{\Gamma_t^i} ds$ of Γ_t^i is constant with respect to time t, i.e., $\frac{g^i(u,t)}{L(\Gamma_t^i)} = \frac{g^i(u,0)}{L(\Gamma_0^i)}, \quad u \in I, t \geq 0$ provided that the total tangential velocity v_T^i satisfies $\partial_{s^i} v_T^i = \kappa^i v_N^i - \frac{1}{L^i}\int_{\Gamma_t^i} \kappa^i v_N^i ds^i$, where v_N^i is the normal velocity in the direction $\mathbf{N^i}$ (see, e.g., [17], [20], [26], [22], [23]). Another suitable choice of the total tangential velocity v_T^i is the so-called asymptotically uniform tangential velocity proposed and analyzed by Mikula and Ševčovič in [22, 23]. It satisfies $\lim_{t\to\infty} \frac{g^i(u,t)}{L(\Gamma_t^i)} = 1$ uniformly with respect to $u \in [0,1]$. This means that the redistribution becomes asymptotically uniform.

In [9], Beneš, Kolář and Ševčovič generalized methodology and techniques of proofs of the local existence, uniqueness and continuation of solutions from our previous paper [8] to the case of combined motion of closed space curves evolving in normal and binormal direction and taking into account mutual nonlocal interactions. We proved the result on existence and uniqueness of classical solutions for a system of n evolving curves in $\mathbb{R}^3$ with mutual nonlocal interactions including, in particular, the vortex dynamics evolved in the normal and binormal directions and external force of the Biot-Savart type, or evolution of interacting dislocation loops.

In the rest of this section we state the result on the existence and uniqueness of classical Hölder smooth solutions to the system of governing equations (2.1). The method of the proof is based on the abstract theory of analytic semi-flows and the theory of maximal regularity in Banach spaces due to Angenent [2, 1]. First, we introduce the function space setting. By $h^{k+\varepsilon}(S^1)$ we denote the so-called little Hölder space, i.e. the Banach space which is the closure of C^∞ smooth functions in the norm Banach space of C^k smooth functions defined on the periodic domain S^1, and such that the k-th derivative is ε-Hölder smooth. Here $0 < \varepsilon < 1$ and k is a non-negative integer. The norm is given as a sum of the C^k norm and the Hölder semi-norm of the k-th derivative. Next, we introduce the scale of Banach spaces of Hölder continuous functions defined in the periodic domain S^1:

$$E_k = (h^{2k+\varepsilon}(S^1))^3, \quad \mathcal{E}_k = \underbrace{E_k \times \ldots \times E_k}_{n-times}, \quad k = 0,\ 1/2,\ 1$$

We assume that the functions $a^i > 0, b^i$, and $\mathbf{F}^i$ are sufficiently smooth and globally Lipschitz continuous functions (see [9, assumtions (H)] for details). Moreover, $\alpha^i, i = 1,\ldots,n$, is the tangential velocity that preserves the relative local length. Assume that the parametrization $\mathbf{X}_0 \equiv (\mathbf{X}_0^i)_{i=1}^n$, of initial curves Γ_0^i belongs to the Hölder space $\mathcal{E}_1$, and it is a uniform parametrization, that is, $|\partial_u \mathbf{X}_0^i(u)| = L(\Gamma_0^i) > 0$ for all $u \in I$ and $i = 1,\ldots,n$. With regard to [9, Theorem 4.1], there exists $T > 0$ and the unique family of curves $\{\Gamma_t^i, t \in [0,T]\}, i = 1,\ldots,n$, evolving in 3D according to the system of nonlinear nonlocal geometric equations (2.1). Their parametrization satisfies $\mathbf{X} = (\mathbf{X}^i)_{i=1}^n \in C([0,T],\mathcal{E}_1) \cap C^1([0,T],\mathcal{E}_0)$, and $\mathbf{X}(\cdot,0) = \mathbf{X}_0$. If the maximal time of existence $T_{max} < \infty$ is finite then $\lim_{t\to T_{max}} \max_{i,\Gamma_t^i} |\kappa^i(\cdot,t)| = \infty$.

3. Flowing finite volumes numerical discretization scheme. In this section, we present a numerical discretization scheme for solving the system of equations (2.1) enhanced by the tangential velocity α^i. Our discretization scheme is based on the method of lines with spatial discretization obtained by means of the finite-volume method. For simplicity, we consider one evolving curve Γ_t (omitting the curve index

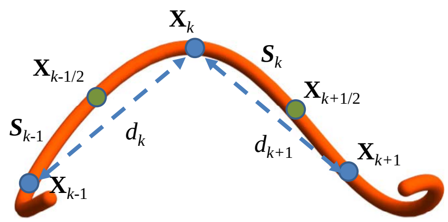

FIG. 3.1. *Discretization of a segment of a 3D curve by the method of flowing finite volumes.*

i) and rewrite the abstract form of (2.1) in terms of the principal parts of its velocity.

$$\partial_t \mathbf{X} = a\partial_s^2 \mathbf{X} + b(\partial_s \mathbf{X} \times \partial_s^2 \mathbf{X}) + \mathbf{F} + \alpha \mathbf{T}. \tag{3.1}$$

We consider M discrete nodes $\mathbf{X}_k = \mathbf{X}(u_k)$, $k = 0, 1, 2, \ldots, M$, $\mathbf{X}_0 = \mathbf{X}_M$ along the curve Γ_t. The dual nodes are defined as $\mathbf{X}_{k\pm\frac{1}{2}} = \mathbf{X}(u_k \pm h/2)$ (see Figure 3.1) where $h = 1/M$, $u_k = kh \in [0, 1]$ and $(\mathbf{X}_k + \mathbf{X}_{k+1})/2$ is the midpoint of the line segment connecting nodes $\mathbf{X}_k$ and $\mathbf{X}_{k+1}$ and differs from $\mathbf{X}_{k\pm\frac{1}{2}} \in \Gamma_t$. The k-th segment $\mathcal{S}_k$ of Γ_t between the nodes $\mathbf{X}_{k+\frac{1}{2}}$ and $\mathbf{X}_{k-\frac{1}{2}}$ represents the finite volume. Integration of equation (3.1) over such a volume yields

$$\begin{aligned}\int_{u_{k-\frac{1}{2}}}^{u_{k+\frac{1}{2}}} \partial_t \mathbf{X} |\partial_u \mathbf{X}| du = \int_{u_{k-\frac{1}{2}}}^{u_{k+\frac{1}{2}}} a \frac{\partial}{\partial_u} \left(\frac{\partial_u \mathbf{X}}{|\partial_u \mathbf{X}|} \right) du + \int_{u_{k-\frac{1}{2}}}^{u_{k+\frac{1}{2}}} b(\partial_s \mathbf{X} \times \partial_s^2 \mathbf{X}) |\partial_u \mathbf{X}| du \\ + \int_{u_{k-\frac{1}{2}}}^{u_{k+\frac{1}{2}}} \mathbf{F} |\partial_u \mathbf{X}| du + \int_{u_{k-\frac{1}{2}}}^{u_{k+\frac{1}{2}}} \alpha \partial_u \mathbf{X} du.\end{aligned} \tag{3.2}$$

Let us denote $d_k = |\mathbf{X}_k - \mathbf{X}_{k-1}|$ for $k = 1, 2, \ldots, M, M + 1$, where $\mathbf{X}_M = \mathbf{X}_0$ and $\mathbf{X}_{M+1} = \mathbf{X}_1$ for closed curve Γ and we approximate the integral expressions in (3.2) by means of the flowing finite volume method as follows:

$$\begin{aligned}
&\int_{u_{k-\frac{1}{2}}}^{u_{k+\frac{1}{2}}} \partial_t \mathbf{X} |\partial_u \mathbf{X}| du \approx \frac{d\mathbf{X}_k}{dt} \frac{d_{k+1} + d_k}{2}, \\
&\int_{u_{k-\frac{1}{2}}}^{u_{k+\frac{1}{2}}} a \partial_u \left(\frac{\partial_u \mathbf{X}}{|\partial_u \mathbf{X}|} \right) du \approx a_k \left(\frac{\mathbf{X}_{k+1} - \mathbf{X}_k}{d_{k+1}} - \frac{\mathbf{X}_k - \mathbf{X}_{k-1}}{d_k} \right), \\
&\int_{u_{k-\frac{1}{2}}}^{u_{k+\frac{1}{2}}} b(\partial_s \mathbf{X} \times \partial_s^2 \mathbf{X}) |\partial_u \mathbf{X}| du \approx b_k \frac{d_{k+1} + d_k}{2} \kappa_k (\mathbf{T}_k \times \mathbf{N}_k), \\
&\int_{u_{k-\frac{1}{2}}}^{u_{k+\frac{1}{2}}} \mathbf{F} |\partial_u \mathbf{X}| du \approx \mathbf{F}_k \frac{d_{k+1} + d_k}{2}, \qquad \int_{u_{k-\frac{1}{2}}}^{u_{k+\frac{1}{2}}} \alpha \partial_u \mathbf{X} du \approx \alpha_k \frac{\mathbf{X}_{k+1} - \mathbf{X}_{k-1}}{2}.
\end{aligned}$$

The approximation of the nonnegative curvature κ (which is regularized by small $0 < \varepsilon \ll 1$ in the case κ_k is close to zero), tangent vector $\mathbf{T}$ and the normal vector $\mathbf{N}$, $\kappa \mathbf{N} = \partial_s \mathbf{T}$ reads as follows:

$$\begin{aligned}
&\kappa_k \approx \left| \frac{2}{d_k + d_{k+1}} \left(\frac{\mathbf{X}_{k+1} - \mathbf{X}_k}{d_{k+1}} - \frac{\mathbf{X}_k - \mathbf{X}_{k-1}}{d_k} \right) \right|, \\
&\mathbf{T}_k \approx \frac{\mathbf{X}_{k+1} - \mathbf{X}_{k-1}}{d_{k+1} + d_k}, \quad \mathbf{N}_k \approx \kappa_k^{-1} \frac{2}{d_k + d_{k+1}} \left(\frac{\mathbf{X}_{k+1} - \mathbf{X}_k}{d_{k+1}} - \frac{\mathbf{X}_k - \mathbf{X}_{k-1}}{d_k} \right).
\end{aligned}$$

To discretize the governing equations, we assume that $\partial_t \mathbf{X}, \partial_u \mathbf{X}, \mathbf{F}, \alpha, \kappa, a, b, \mathbf{T}$ and $\mathbf{N}$ are constant over the finite volume $\mathcal{S}_k$ between the nodes $\mathbf{X}_{k-\frac{1}{2}}$ and $\mathbf{X}_{k+\frac{1}{2}}$, taking values $\partial_t \mathbf{X}_k, \partial_u \mathbf{X}_k, \mathbf{F}_k, \alpha_k, \kappa_k, \mathbf{T}_k$ and $\mathbf{N}_k$, respectively. In approximation $\mathbf{F}_k$ of the non-local vector-valued function $\mathbf{F}$, we assume that the curve Γ entering the definition of $\mathbf{F}$ is approximated by the polygonal curve with vertices $(\mathbf{X}_0, \mathbf{X}_1, \ldots, \mathbf{X}_M)$. To find the approximation α_k of the tangential velocity, we apply a simple trapezoidal integration formula as in [27]. The values $\alpha_0 = \alpha_M$ are chosen so that $\sum_{j=1}^{M} \alpha_j d_j = 0$. In summary, the semi-discrete scheme for solving (3.1) can be written as follows.

$$
\begin{aligned}
\frac{d\mathbf{X}_k}{dt}\frac{d_{k+1}+d_k}{2} &= a_k\left(\frac{\mathbf{X}_{k+1}-\mathbf{X}_k}{d_{k+1}} - \frac{\mathbf{X}_k-\mathbf{X}_{k-1}}{d_k}\right) + b_k\frac{d_{k+1}+d_k}{2}\kappa_k(\mathbf{T}_k\times\mathbf{N}_k)\\
&\quad +\mathbf{F}_k\frac{d_{k+1}+d_k}{2} + \alpha_k\frac{\mathbf{X}_{k+1}-\mathbf{X}_{k-1}}{2},\\
\mathbf{X}_k(0) &= \mathbf{X}_{ini}(u_k), \quad \text{for } k = 1,\ldots,M.
\end{aligned}
$$

Resulting system of ODEs is solved numerically by means of the 4th-order explicit Runge-Kutta-Merson scheme with automatic time stepping control and the tolerance parameter 10^{-3} (see [25]). We chose the initial time step as $4h^2$, where $h = 1/M$ is the spatial mesh size.

4. Examples of evolution of linked Fourier curves under Biot-Savart external force. As an example of a non-local source term $\mathbf{F}$ we consider the external force corresponding to the Biot-Savart law. It represents the integrated influence of all points belonging to the curve $\Gamma_t = \{\mathbf{X}(s), s \in [0, L(\Gamma_t)]\}$ at a given point $\mathbf{X} \in \mathbb{R}^3, \mathbf{X} \notin \Gamma_t$. It is given as a line integral:

$$
\mathbf{F}(\mathbf{X}, \Gamma_t) = \int_{\Gamma_t} \frac{(\mathbf{X}-\mathbf{X}(s))\times\partial_s\mathbf{X}(s)}{|\mathbf{X}-\mathbf{X}(s)|^3} ds. \tag{4.1}
$$

Let Γ_t^1 and Γ_t^2 be two non-intersecting closed curves in 3D. The Biot-Savart force is connected with the Gauss linking number and the integral $\mathrm{link}(\Gamma_t^1, \Gamma_t^2)$ of Γ_t^1 and Γ_t^2 can be defined as follows:

$$
\begin{aligned}
\mathrm{link}(\Gamma_t^1, \Gamma_t^2) &= \frac{1}{4\pi}\oint_{\Gamma_t^1}\oint_{\Gamma_t^2} \frac{\det\left(\partial_{s_1}\mathbf{X}^1(s_1), \partial_{s_2}\mathbf{X}^2(s_2), \mathbf{X}^1(s_1)-\mathbf{X}^2(s_2)\right)}{|\mathbf{X}^1(s_1)-\mathbf{X}^2(s_2)|^3} ds_1 ds_2\\
&= -\frac{1}{4\pi}\oint_{\Gamma_t^1} \mathbf{F}(\mathbf{X}^1(s_1), \Gamma_t^2)\cdot\partial_{s_1}\mathbf{X}^1(s_1) ds_1 = -\frac{1}{4\pi}\oint_{\Gamma_t^2} \mathbf{F}(\mathbf{X}^2(s_2), \Gamma_t^1)\cdot\partial_{s_2}\mathbf{X}^2(s_2) ds_2,
\end{aligned}
$$

where the closed curves Γ_t^1 and Γ_t^2 are parameterized by $\mathbf{X}^1(s_1)$ and $\mathbf{X}^2(s_2)$, respectively. The linking number $\mathrm{link}(\Gamma_t^1, \Gamma_t^2)$ belongs to $\mathbb{Z}$.

A Fourier curve is a closed curve in 3D that can be parameterized by a finite Fourier series in the parameter $u \in [0,1]$. In Fig. 4.1 a) we show two linked circles Γ_t^1 and Γ_t^2 with the linking number $\mathrm{link}(\Gamma_t^1, \Gamma_t^2) = -1$ for parameterization (4.2), and $\mathrm{link}(\Gamma_t^1, \Gamma_t^2) = 1$ when parameterized by (4.3):

$$
\mathbf{X}^1(u) = (\cos(2\pi u), \sin(2\pi u), 0), \quad \mathbf{X}^2(u) = (1+\cos(2\pi u), 0, \sin(2\pi u)), \tag{4.2}
$$
$$
\mathbf{X}^1(u) = (-\sin(2\pi u), \cos(2\pi u), 0), \mathbf{X}^2(u) = (1+\cos(2\pi u), 0, -\sin(2\pi u)). \tag{4.3}
$$

In Fig. 4.1 b) we present two linked circles given by (4.3), and Biot-Savart force vector field (4.1) induced by Γ_t^2 acting on points belonging to Γ_t^1.

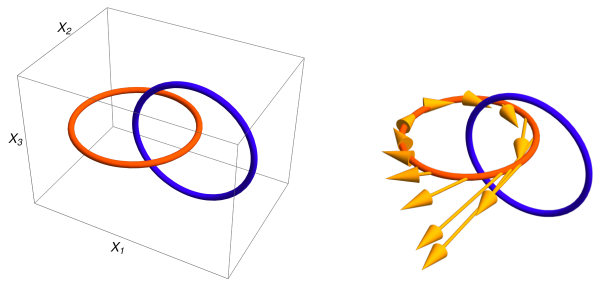

a) b)

FIG. 4.1. *Two linked circles a) and the Biot-Savart force vector field induced by Γ_t^2 acting on points of Γ_t^1, b).*

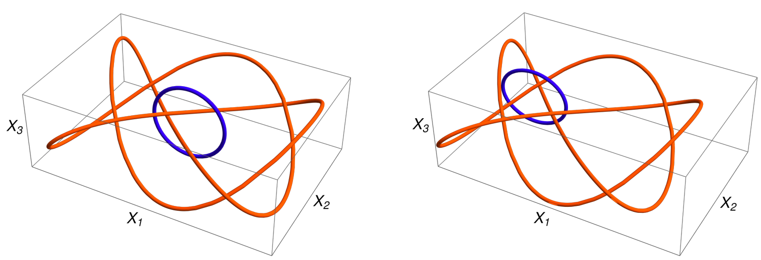

a) b)

FIG. 4.2. *The Listing's 8-knot curve linked with a circle a) and an ellipse b).*

The explicit parametrization of the Listing's 8-knot curve $\mathbf{X}^1$ is given by

$$\mathbf{X}^1(u) = (3\cos(4\pi u), 2\sin(6\pi u + 1/2), (\cos(10\pi u + 1/2) + \sin(6\pi u + 1/2))/2). \quad (4.4)$$

The Listing's 8-knot curve parameterized by (4.4) is shown in Fig. 4.2 a) with a linked-in circle (linking number 0) that is parameterized by:

$$\mathbf{X}^2(u) = (\cos(2\pi u),\ 0\ , \sin(2\pi u)). \quad (4.5)$$

The Listing's 8-knot curve Γ_t^1 with a linked-in ellipse (linking number -2) that is parameterized by:

$$\mathbf{X}^2(u) = (\cos(2\pi u) - 1.5,\ 0.5\ , 0.8\sin(2\pi u)) \quad (4.6)$$

is shown in Fig. 4.2 b).

In what follows, we present results of numerical approximation of solutions to the coupled system of governing PDEs:

$$\begin{aligned} \partial_t \mathbf{X}^1 &= \partial_{s^1}^2 \mathbf{X}^1 + \delta \mathbf{F}(\mathbf{X}^1, \Gamma_t^2), \\ \partial_t \mathbf{X}^2 &= \partial_{s^2}^2 \mathbf{X}^2 + \delta \mathbf{F}(\mathbf{X}^2, \Gamma_t^1), \end{aligned}$$

which is subject to initial conditions $\mathbf{X}^1(\cdot, 0)$ and $\mathbf{X}^2(\cdot, 0)$ at the origin $t = 0$. As a forcing term, we consider the Biot-Savart force $\mathbf{F}(\mathbf{X}^i, \Gamma_t^j)$ scaled by the factor $\delta = 0.1$.

In Fig. 4.3 and Fig. 4.4 we present the time evolution of two linked circles Γ_t^1 and Γ_t^2 parameterized by (4.2) with the linking number $\mathrm{link}(\Gamma_t^1, \Gamma_t^2) = -1$ and $\mathrm{link}(\Gamma_t^1, \Gamma_t^2) = 1$, respectively.

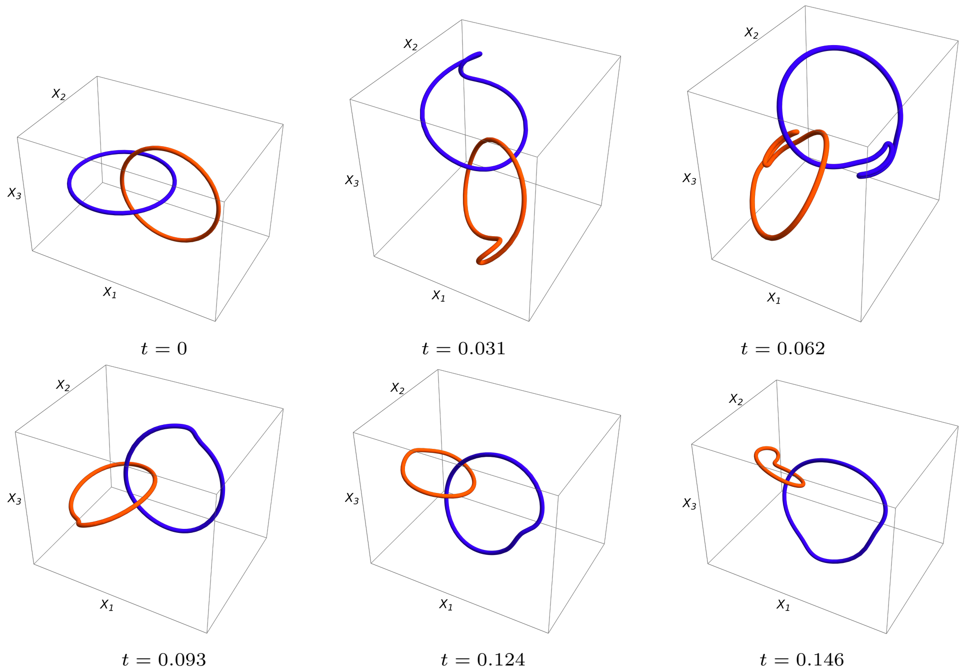

FIG. 4.3. *Evolution of the initial linked circles parameterized by (4.2) with link*$(\Gamma_t^1, \Gamma_t^2) = -1$.

In Fig. 4.5 we present the time evolution of the initial Listing's 8-curve Γ_t^1 linked with a circle Γ_t^2 parameterized by (4.5) shown in Fig. 4.2 a) with the linking number $\text{link}(\Gamma_t^1, \Gamma_t^2) = 0$. In Fig. 4.6 we present the time evolution of the initial Listing's 8-curve Γ_t^1 linked with an ellipse Γ_t^2 parametrized by (4.6) shown in Fig. 4.2 b) with the linking number $\text{link}(\Gamma_t^1, \Gamma_t^2) = -2$.

5. Conlusions. In this article, we investigated a set of geometric evolution equations that describe the curvature-driven motion of a family of 3D curves along the normal and binormal directions. An evolving family of curves can interact in either local or non-local ways. In particular, we analyzed evolving pairs of closed linked curves that form knots in 3D. We utilized the direct Lagrangian method to solve the geometric flow of these interacting curves. We applied the abstract theory of nonlinear analytic semi-flows to prove the local existence, uniqueness, and continuation of classical Hölder smooth solutions for the system of nonlinear parabolic equations in question. Using the finite-volume method, we proposed an effective numerical method for solving the governing system of parabolic partial differential equations. Finally, we provided multiple computational studies on the flow of linked curves.

Acknowledgments. The first author received partial support from the project 21-09093S of the Czech Science Foundation. The second author received support from the Slovak Research and Development Agency project APVV-20-0311.

REFERENCES

[1] S. ANGENENT, *Parabolic equations for curves on surfaces. I: Curves with p-integrable curvature*, Ann. Math., 132(2) (1990), pp. 451–483.

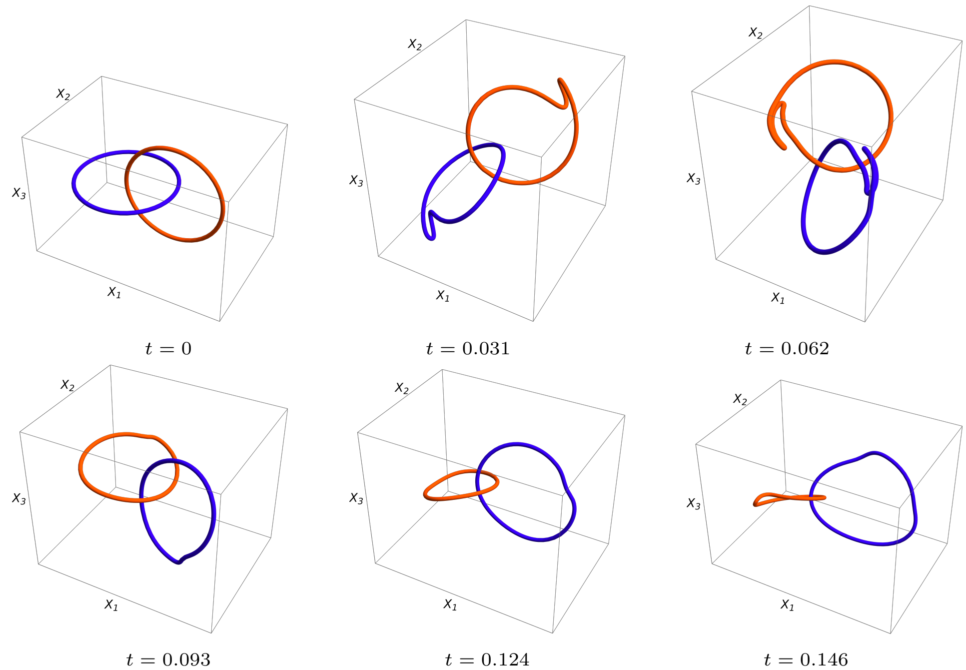

FIG. 4.4. *Evolution of the initial linked circles parameterized by (4.3).*

[2] S. Angenent, *Nonlinear analytic semi-flows.* Proc. R. Soc. Edinb., Sect. A, 115 (1990), pp. 91–107.

[3] R.J. Arms and F. R. Hama, *Localized Induction Concept on a Curved Vortex and Motion of an Elliptic Vortex Ring*, Phys. Fluids, 8 (1965), pp. 553-559.

[4] J. W. Barrett, H. Garcke, and R. Nürnberg, *Numerical approximation of gradient flows for closed curves in R^d*, IMA J. Numer. Anal., 30(1), (2010), pp. 4–60.

[5] J. W. Barrett, H. Garcke, and R. Nürnberg, *Parametric approximation of isotropic and anisotropic elastic flow for closed and open curves*, Numer. Math., 120(3), (2012), pp. 489–542.

[6] R. Betchov, *On the curvature and torsion of an isolated vortex filament*, J. Fluid Mech., 22 (1965), pp. 471-479.

[7] G. P. Bewley, M. S. Paoletti, K. R. Sreenivasan, and D. P. Lathrop, *Characterization of reconnecting vortices in super-fluid helium*, P. Natl. Acad. Sci. USA., 105(37) (2008), pp. 13707-13710.

[8] M. Beneš, M. Kolář M, and D. Ševčovič, *Curvature driven flow of a family of interacting curves with applications*, Math. Method. Appl. Sci., 43 (2020), pp. 4177-4190.

[9] M. Beneš, M. Kolář M, and D. Ševčovič, *Qualitative and numerical aspects of a motion of a family of interacting curves in space*, SIAM Journal on Applied Mathematics, 82(2), (2022), 549-575.

[10] M. Minárik, M. Beneš, and J. Kratochvíl, *Simulation of dynamical interaction between dislocations and dipolar loops*, Journal of Applied Physics, 107(2), (2010), 061802.

[11] J. Křišťan, J. Kratochvíl, M. Minárik and M. Beneš, *Simulation of dynamical interacting dislocations glide in a channel of persistent slip band*, Modeling and Simulation in Material Science and Engineering, 17, (2009), 045009.

[12] Ch. M. Elliott and H. Fritz, *On approximations of the curve shortening flow and of the mean curvature flow based on the DeTurck trick*, IMA J. Numer. Anal., 37(2), (2017), pp. 543–603.

[13] Y. Fukumoto, *On Integral Invariants for Vortex Motion under the Localized Induction Approximation*, J. Phys. Soc. Jpn., 56(12) (1987), pp. 4207–4209.

[14] Y. Fukumoto and T. Miyzaki *Three-dimensional distortions of a vortex filament with axial velocity*, J. Fluid Mech., 222 (1991), pp. 369–416.

[15] H. Garcke, Y. Kohsaka, and D. Ševčovič, *Nonlinear stability of stationary solutions for*

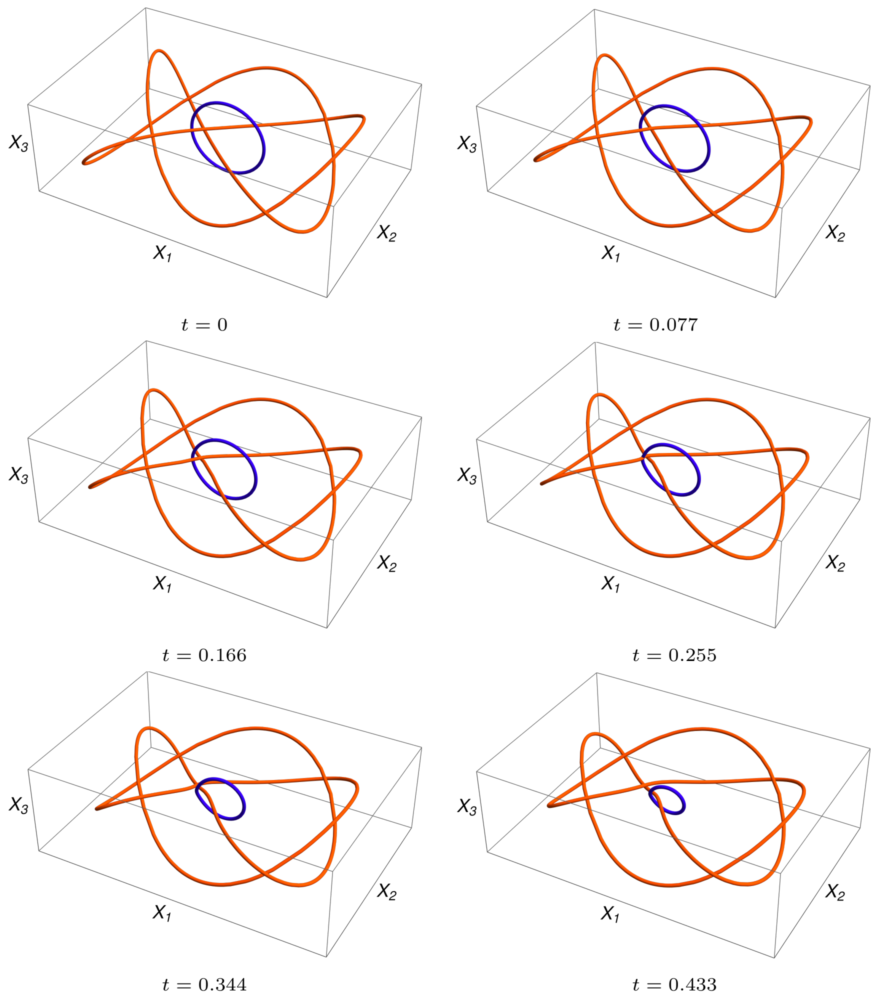

FIG. 4.5. *Evolution of the initial Listing's 8-curve (4.4) linked with a circle (blue). (4.5) The external force acting on both curves is given by the regularized Biot-Savart force given by (4.1).*

curvature flow with triple junction, Hokkaido Math. J., 38(4) (2009), pp. 721–769.

[16] H. Helmholtz, *Über Integrale der hydrodynamischen Gleichungen, welche den Wirbelbewegungen entsprechen*, J. Reine Angew. Math., 55 (1858), pp. 25–55.

[17] T. Y. Hou, J. Lowengrub, and M. Shelley, *Removing the stiffness from interfacial flows and surface tension*, J. Comput. Phys., 114 (1994), pp. 312–338.

[18] F. de la Hoz and L. Vega, *Vortex filament equation for a regular polygon*, Nonlinearity, 27(12) (2014), pp. 3031–3057.

[19] D. A. Kessler, J. Koplik, and H. Levine, *Numerical simulation of two-dimensional snowflake growth*, Phys. Rev. A, 30(5), (1984), pp. 2820–2823.

[20] M. Kimura, *Numerical analysis for moving boundary problems using the boundary tracking method*, Jpn. J. Indust. Appl. Math., 14 (1997), pp. 373–398.

[21] R. Mariani and K. Kontis, *Experimental studies on coaxial vortex loops*, Phys. Fluids, 22 (2010), p. 126102.

[22] K. Mikula and D. Ševčovič, *Computational and qualitative aspects of evolution of curves driven by curvature and external force*, Comput. Vis. Sci., 6 (2004), pp. 211–225.

[23] K. Mikula and D. Ševčovič, *A direct method for solving an anisotropic mean curvature flow of plane curves with an external force*, Math. Methods Appl. Sci., 27 (2004), pp. 1545–1565.

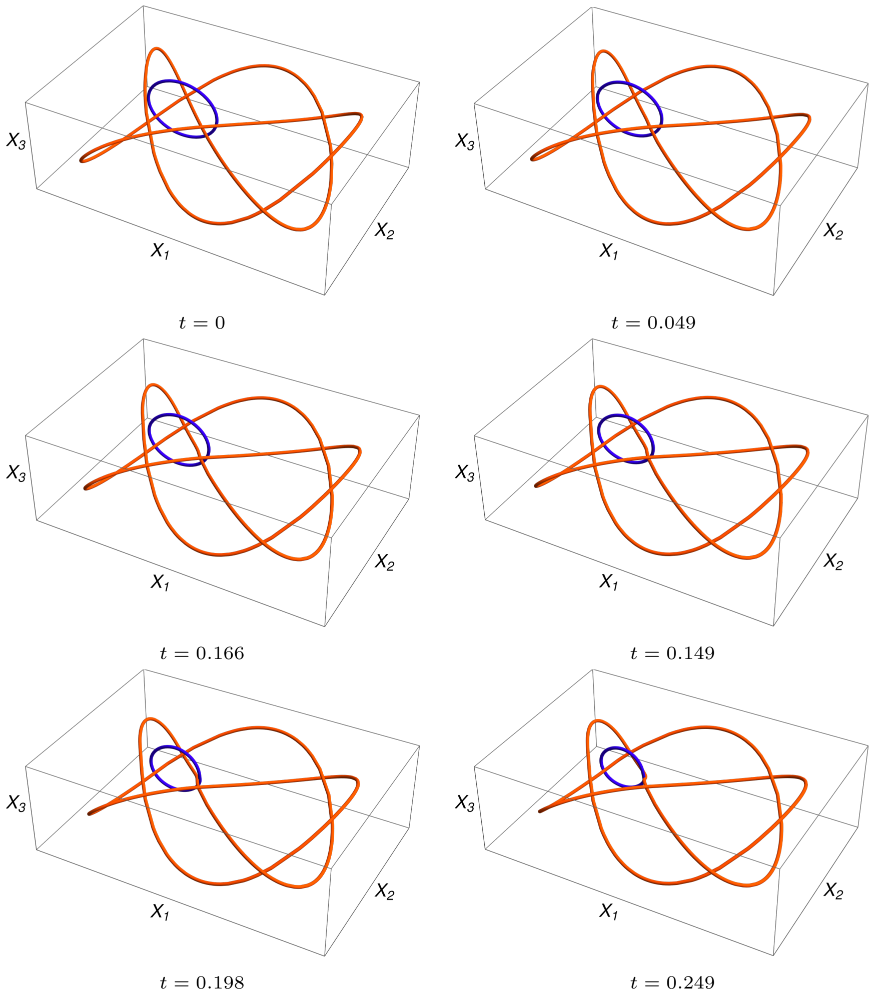

FIG. 4.6. *Evolution of the initial Listing's 8-curve linked with an ellipse (blue) (4.6). The external force acting on both curves is given by the regularized Biot-Savart force given by (4.1).*

[24] L. S. DA RIOS, *Sul Moto di un filetto vorticoso di forma qualunque*, Rend. Circ. Mat. Palermo, 22 (1906), pp. 117-135.

[25] P. PAUŠ, M. BENEŠ, M. KOLÁŘ, AND J. KRATOCHVÍL, *Dynamics of dislocations described as evolving curves interacting with obstacles*, Model. Simul. Mater. Sci., 24 (2016), p. 035003.

[26] K. MIKULA AND D. ŠEVČOVIČ, *Evolution of plane curves driven by a nonlinear function of curvature and anisotropy*, SIAM J. Appl. Math., 61 (2001), pp.1473–1501.

[27] D. ŠEVČOVIČ AND S. YAZAKI, *Computational and qualitative aspects of motion of plane curves with a curvature adjusted tangential velocity*, Math. Methods Appl. Sci., 35 (2012), pp. 1784–1798.

[28] J. STRAIN, *A boundary integral approach to unstable solidification*, J. Comput. Phys., 85(2), (1989), pp. 342–389.

[29] W. THOMSON, *On Vortex Atoms*, Proc. R. Soc. Edinb., 6 (1867), 94–105.

[30] L. VEGA, *The dynamics of vortex filaments with corners*, Commun. Pur. Appl. Anal., 14(4) (2015), 1581–1601.